

## Low-Temperature Anomalies and Ferromagnetism of $\text{EuB}_6$

L. Degiorgi,<sup>1</sup> E. Felder,<sup>1</sup> H. R. Ott,<sup>1</sup> J. L. Sarrao,<sup>2</sup> and Z. Fisk<sup>2</sup>

<sup>1</sup>Laboratorium für Festkörperphysik, ETH Hönggerberg, 8093 Zürich, Switzerland

<sup>2</sup>National High Magnetic Field Laboratory, Florida State University, 1800 Paul Dirac Drive, Tallahassee, Florida 32306

(Received 21 April 1997)

Measurements of the specific heat  $C_p(T)$  of single-crystalline  $\text{EuB}_6$  reveal that the magnetically ordered ground state of this compound is reached via two consecutive phase transitions with onsets at 16 and 14 K, respectively. These transitions provoke a substantial change in the IR spectral range of the electronic excitation spectrum as evidenced by measurements of the optical reflectivity over a wide spectral range and at temperatures between 6 K and room temperature. The data analysis suggests that the magnetic ordering of  $\text{EuB}_6$  inflicts a highly unusual alteration of its electronic excitation spectrum. [S0031-9007(97)04851-5]

PACS numbers: 75.40.Cx, 78.20.-e, 75.30.Kz

$\text{EuB}_6$  is a cubic compound with a unit cell that contains the Eu cation in the center of the cube surrounded by eight boron octahedra centered at the corners of the cube. It orders ferromagnetically at low temperatures [1,2] and the Curie temperature  $T_C$  is found to be quite sensitive to the chemical composition of the material. Below  $T_C$  the electrical resistivity is drastically reduced and a very large negative magnetoresistance above and, even more so, below the ferromagnetic transition of  $\text{EuB}_6$  was observed [3]. In this Letter we report on the observation of anomalies related with the magnetic ordering, in particular in the temperature dependence of the specific heat  $C_p(T)$  and in the optical reflectivity  $R(\omega, T)$ . The  $C_p(T)$  data reveal the occurrence of at least two phase transitions at and below  $T_C = 16$  K. The optical data reveal substantial frequency shifts of a plasma edge feature in  $R(\omega)$ . With decreasing temperature we first note a redshift above  $T_C$ , followed by a giant blueshift concomitant with the onset of magnetic ordering.

These observations seem of general interest because recent experimental and theoretical activities in solid state physics have been focused on the investigation and the understanding of very large changes of the electrical resistivity  $\rho$  upon the application of an external magnetic field. Particularly intriguing is the case of a series of manganese oxides with compositions  $\text{La}_{1-x}\text{AE}_x\text{MnO}_3$ , where AE is an alkaline earth element. It has long been known that [4,5], for a limited range of  $x$ , these materials undergo a phase transition to a ferromagnetic state below room temperature, the Curie temperature  $T_C$  varying with  $x$ . It was established that the temperature dependence of the resistivity  $\rho$  is of semiconducting character in the paramagnetic state with an abrupt change to metallic behavior upon the onset of the ferromagnetic order, revealed by reductions of the electrical resistivity by orders of magnitude. More recently it has been demonstrated that, at temperatures close to but below  $T_C$ , very large reductions of  $\rho$  may also be achieved by external magnetic fields, and the notion of colossal magnetoresistance has been in-

roduced [6]. Recent experiments [7] revealing a strong dependence of the Curie temperature on the mass of different oxygen isotopes  $^{16}\text{O}$  and  $^{18}\text{O}$  seem to support the view that a fairly strong coupling between electrons and the lattice is needed to fully describe the experimental observations [8,9]. For  $\text{EuB}_6$ , substantial shifts of  $T_C$  may be accomplished by applying external mechanical pressure [3] suggesting that, also in this case, the electron lattice coupling may be substantial.

The compounds  $\text{RE}^{3+}\text{B}_6$ , where RE is a rare-earth element, are usually metals,  $\text{LaB}_6$  being a typical example of this type of materials and claimed to be a superconductor below 0.122 K [10]. Less obvious is the situation for the hexaborides of the type  $\text{AE}^{2+}\text{B}_6$ , with AE being an alkaline-earth element. Although it might be expected that these compounds are semiconductors, recent experiments have shown that the variation of  $\rho(T)$  of  $\text{SrB}_6$  is rather complicated, resulting in a metallic state at very low temperatures [11]. Band structure calculations confirm that the electronic excitation spectrum is extremely dependent on the dimensions of the Boron octahedra, with zero or nonzero overlap of the valence and conduction bands at the X point of the Brillouin zone [12]. For  $\text{Eu}^{2+}\text{B}_6$ , for some time claimed to be a semiconductor [13];  $\rho(T)$  definitely reveals metallic behavior below 300 K [3].

The Curie temperature of  $\text{EuB}_6$  is an order of magnitude smaller than those of the manganites and, while the magnetic moments in the hexaboride materials are localized on the  $\text{Eu}^{2+}$  ions, they presumably are of more itinerant character in the manganites. In spite of these differences, we aimed at identifying common features of these materials. In particular, we searched for possible relations between the magnetic ordering and the accompanying strong variations of  $\rho(T)$ , as well as for indications of the role of the crystal lattice in influencing these phenomena.

Both the specific heat and the optical measurements were made on the same single crystalline specimen in the form of a platelet with dimensions of  $3.7 \times 1.6 \times 0.2 \text{ mm}^3$  and 3.5 mg weight. The sample was

extracted from a batch of crystals that were grown from Al flux, using  $\text{EuB}_6$  powder that was prepared by borothermal reduction of  $\text{Eu}_2\text{O}_3$ . Hexaboride samples grown by this method have been shown to be of exceptional quality with regard to both structure and chemical composition [11]. The specific heat was measured with a thermal relaxation method between 0.07 and 19 K. The optical reflectivity at various temperatures was measured from the far infrared (FIR) to the ultraviolet part of the spectrum. Details of the experimental setup have previously been described [11]. The optical conductivity  $\sigma_1(\omega, T)$  was evaluated via the Kramers-Kronig transformation of the reflectivity spectra. Recent measurements of the electrical resistivity  $\rho$  in zero and nonzero magnetic field on samples obtained with the same preparation technique confirmed the large reduction of  $\rho$  below 16 K in zero field and upon applying an external magnetic field in the same range of temperature [14].

In Fig. 1 we present the  $C_p(T)$  data between 0.07 and 19 K. Although on a rough scale they are similar to previously published results [5,6], they differ in some important details. A small but distinct anomaly indicates the onset of a transition at about 16 K, a feature in  $C_p(T)$  that has not been resolved in previous experiments. A much larger specific heat anomaly sets in at 14 K but the maximum  $C_p$  value is reached only at 10.5 K. A width of a few kelvins of this dominant anomaly has been observed in earlier measurements [15,16] and it seems to be an intrinsic feature of this transition. Our data indicate that also in the range of 4 K yet another transition might occur. This feature is much more evident on plots with other scales but will be discussed in more detail elsewhere. At very low temperatures we identify the onset of a Schottky anomaly due to the splitting of the energy levels of  $^{151}\text{Eu}$  and  $^{153}\text{Eu}$  nuclei in the internal magnetic field provided by the ordered moments. The molar entropy involved in the transitions up to 16 K is, to a very good approximation, identical with  $R \ln 8$ , the expected value for divalent Eu ions.

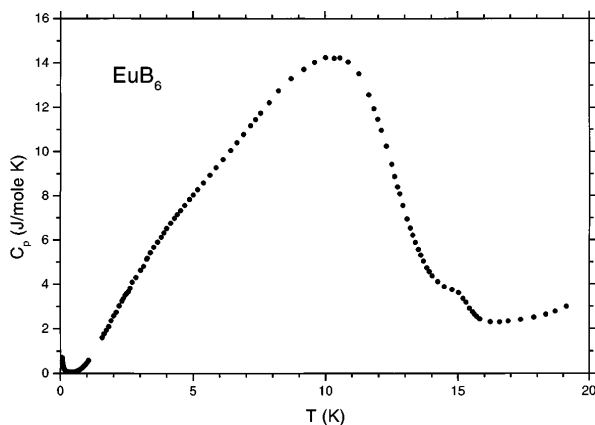


FIG. 1. Temperature dependence of the specific heat of  $\text{EuB}_6$  between 0.07 and 19 K.

Figure 2 presents the reflectivity spectra at several temperatures above and below  $T_C$ , particularly emphasizing the temperature variation of the steep drop in  $R(\omega)$  that we interpret as a plasma edge type behavior. The plasma edge and the corresponding minimum in  $R(\omega)$  define the so-called “screened” plasma frequency. With decreasing temperature this feature first shifts towards low frequencies (redshift) above  $T_C$ , followed by a substantial shift towards higher frequencies (blueshift) at and below the ferromagnetic transition. This type of a solely temperature-induced giant optical effect has, to our knowledge, not been observed before. For comparison we recall that in the  $\text{La}_{1-x}\text{Sr}_x\text{MnO}_3$  series, respectable blueshifts of the plasma edge are obtained by increasing the Sr concentration thereby inducing an insulator to metal transition [17]. A similar, again doping induced plasma edge shift has been observed in  $\text{Sr}_{14-x}\text{Ca}_x\text{Cu}_{24}\text{O}_{41}$  ladder compounds [18].

Figures 3(a) and 3(b) emphasize the spectral ranges around two excitations at  $145$  and  $850$   $\text{cm}^{-1}$ , respectively. The mode at  $145$   $\text{cm}^{-1}$  reveals an optical phonon due to the relative motion between the Eu ions and the B octahedra, its frequency scaling perfectly with the optical phonon found in  $\text{SrB}_6$  using simple reduced mass arguments [11]. The mode at  $850$   $\text{cm}^{-1}$  most likely originates in vibrations of the B octahedra. Both modes are only weakly affected by the magnetic transition at  $T_C$ . The mode at  $145$   $\text{cm}^{-1}$  does not change its frequency at all; the one at  $850$   $\text{cm}^{-1}$  slightly shifts towards higher frequencies upon the onset of magnetic order, implying at least some coupling of electronic and lattice degrees of freedom.

The corresponding real part  $\sigma_1(\omega)$  of the optical conductivity in the FIR spectral range is displayed in Fig. 4. We note a low frequency metallic component in the form of increasing conductivity as  $\omega$  tends to zero,

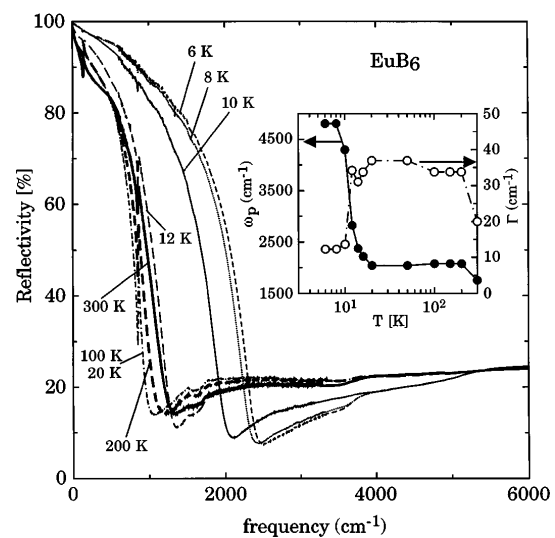


FIG. 2. Reflectivity  $R(\omega)$  spectra of  $\text{EuB}_6$  in the FIR and MIR spectral range at various temperatures between 6 and 300 K. The inset shows  $\omega_p(T)$  and  $\bar{\Gamma}(T)$  (see text).

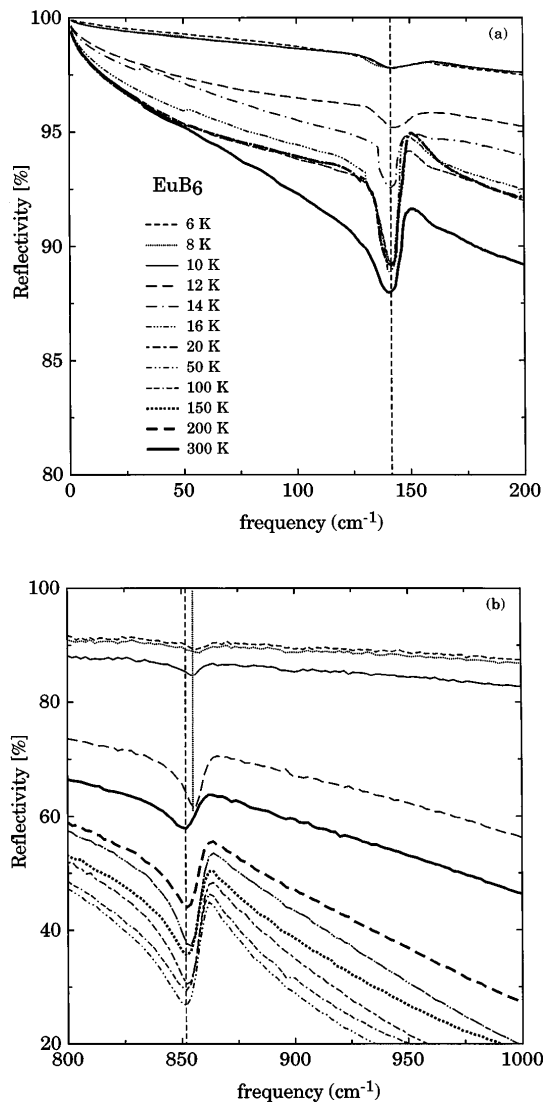


FIG. 3. Magnified parts of the reflectivity  $R(\omega)$  between (a) 0 and 200  $\text{cm}^{-1}$  and (b) 800 and 1000  $\text{cm}^{-1}$ , respectively.

and the FIR optical phonon mode. The inset of Fig. 4 shows the complete  $\sigma_1$  spectrum at room temperature, also revealing the high frequency electronic interband transitions [19].

For the analysis of the excitation spectra we model both  $R(\omega)$  and  $\sigma_1(\omega)$  using the classical Lorentz-Drude dispersion theory [20]. In spite of its phenomenological character, this type of analysis is very instructive for distributing the total spectral weight among the various components and for establishing the temperature dependence of important parameters such as the unscreened plasma frequency  $\omega_p$  and the scattering rate  $\Gamma$ . Details about the fit procedure will be presented and discussed elsewhere. At each temperature the spectrum is well reproduced by considering a Drude-type component due to itinerant charge carriers and five harmonic oscillators (HO) representing phonon modes and high

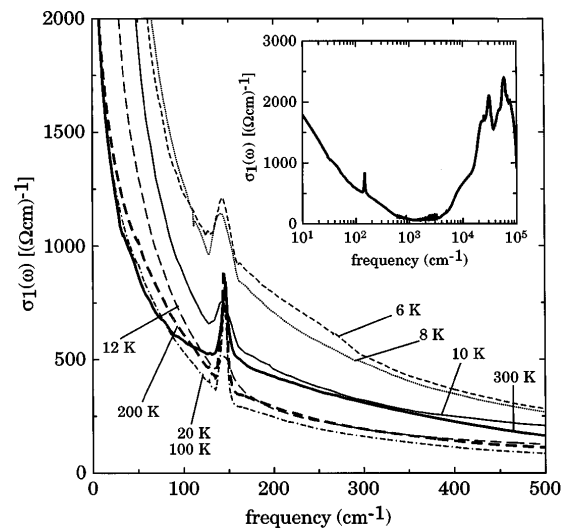


FIG. 4. FIR optical conductivity between 0 and 500  $\text{cm}^{-1}$  at various temperatures. The inset shows the complete  $\sigma_1(\omega)$  spectrum and 300 K.

frequency electronic interband transitions. For a full account of the signal of the metallic contribution in the MIR-FIR spectral range, however, the simple Drude component has to be augmented by an additional HO centered at a frequency of 100  $\text{cm}^{-1}$ . The total number of components was chosen to be the same at all temperatures. The fitting procedures lead to numerically consistent results and distinct temperature dependences of the Drude parameters  $\omega_p$  and  $\Gamma$ , as well as the mode strengths of the HO. The resonance frequencies and the corresponding damping parameters are almost temperature independent. Since the total spectral weight of  $\sigma_1(\omega)$  is temperature independent, the distinct temperature dependencies of both  $R(\omega)$  and  $\sigma_1(\omega)$ , particularly in the vicinity of  $T_C$ , are due to redistributions of spectral weight between the different components.

The temperature dependences of  $\omega_p$  and of  $\Gamma$  are shown in the inset of Fig. 2. In spite of the redshift of the plasma edge in  $R(\omega)$  with decreasing temperature above  $T_C$ ,  $\omega_p$  slightly increases below 300 K. In addition to a spectral-weight redistribution from the FIR absorption at 100  $\text{cm}^{-1}$  to interband transitions at approximately 1200 and 2500  $\text{cm}^{-1}$ , a slight enhancement of  $\omega_p$  is necessary to keep the quality of the fit to the experimental  $R(\omega)$  curve. Although the FIR reflectivity increases steadily with decreasing temperature, the scattering rate  $\Gamma$  also increases, displaying a broad maximum between 100 K and  $T_C$ . Below  $T_C$ ,  $\omega_p$  first increases smoothly but then more steeply below the second transition at 14 K, reaching a constant value around 8 K. The sharp decrease of  $\Gamma$  below  $T_C$  is expected because of the reduced spin flip scattering. The giant plasma edge shift below  $T_C$  is the result of an almost complete weight shift from the excitation at 2500  $\text{cm}^{-1}$  to the modes at 100 and

1200  $\text{cm}^{-1}$ , and the Drude component, respectively, a feature whose interpretation is not obvious to us.

Of particular interest is the hidden broad absorption centered at approximately 100  $\text{cm}^{-1}$  which leads to the “nonsimple” Drude behavior in the FIR spectral range. It occurs at all temperatures and gains in strength below  $T_C$ . There is no obvious reason to associate this mode with a phonon. The width of the mode also rules out the possibility of a defect induced phonon excitation. However, the interplay of a phonon mode with the plasma excitation of the itinerant charge carriers might lead to a collective plasmon-phonon mode. The observation of such a mode, usually occurring between the acoustic and the optical phonon branches, has previously been claimed for  $\text{SmB}_6$  [21]. A similar feature has recently been identified in  $\text{SrB}_6$  [11] at approximately 40  $\text{cm}^{-1}$  and was tentatively ascribed to some defect-induced excitation. In the present case the weight gain of this mode below  $T_C$  is not *a priori* a favorable argument for this type of explanation.

The charge dynamics spectra of  $\text{EuB}_6$  and of  $\text{La}_{1-x}\text{Sr}_x\text{MnO}_3$  materials are quite different. The huge transfer of spectral weight from high to lower frequencies with decreasing temperature, as observed in the manganites [22], is replaced by a more subtle redistribution of mode strengths in the MIR spectral range for  $\text{EuB}_6$ . This might simply be the result of the difference in energy scales relevant for the electronic and magnetic phenomena in the two types of materials. Common to both cases is the only qualitative scaling of  $\omega_p^2$  with the square of the magnetization  $M_s$  representing the moment polarization in the mean field approximation. This could indicate that also in  $\text{EuB}_6$  the dynamics of the magnetic moments affects the electronic excitations via mutual strong coupling as was suggested for the case of the manganites [22].

The magnetic ordering in  $\text{EuB}_6$  is not of simple character and occurs via two consecutive transitions, invoking considerable changes in the electronic excitation spectrum of this compound. Below  $T_C$  the unscreened plasma frequency increases considerably, suggesting an increase of the itinerant charge carrier concentration, a reduction of their effective mass or a combination of the two, both driven by the onset of magnetic order. This feature is not expected considering the almost identical calculated electronic structures in the paramagnetic and ferromagnetic state of  $\text{EuB}_6$ , respectively [12], and therefore, additional interactions not included in band structure calculations must play an important role. Resolving this puzzle and explaining the above-mentioned spectral-weight shift upon magnetic ordering seems to be a challenging task for the future.

We thank J. Müller for technical assistance. L.D. would like to thank P. Wachter for his generous support in providing infrastructure related with these experiments.

The work at ETH Zürich benefited from financial support of the Schweizerische Nationalfonds zur Förderung der wissenschaftlichen Forschung. J.L.S. and Z.F. acknowledge a financial grant offered by the Japanese New Energy and Development Organization (NEDO).

- 
- [1] B. T. Matthias, T. H. Geballe, K. Andres, E. Corenzwit, G. W. Hull, and J. P. Maita, *Science* **159**, 530 (1968).
  - [2] M. Kasaya, J. M. Tarascon, J. Etourneau, and P. Hagenmuller, *Mater. Res. Bull.* **13**, 751 (1978).
  - [3] C. N. Guy, S. von Molnar, J. Etourneau, and Z. Fisk, *Solid State Commun.* **33**, 1055 (1980).
  - [4] G. H. Jonker and J. H. Van Santen, *Physica (Utrecht)* **16**, 337 (1950).
  - [5] J. H. Van Santen and G. H. Jonker, *Physica (Utrecht)* **16**, 599 (1950).
  - [6] S. Jin, T. H. Tiefel, M. McCormack, R. A. Fastnacht, R. Ramesh, and L. H. Chen, *Science* **264**, 413 (1994).
  - [7] G. M. Zhao, K. Conder, H. Keller, and K. A. Müller, *Nature (London)* **381**, 676 (1996).
  - [8] A. J. Millis, P. B. Littlewood, and B. I. Shraiman, *Phys. Rev. Lett.* **74**, 5144 (1995).
  - [9] A. J. Millis, B. I. Shraiman, and R. Mueller, *Phys. Rev. Lett.* **77**, 175 (1996).
  - [10] A. J. Arko, G. Crabtree, J. B. Ketterson, F. M. Müller, P. F. Walch, L. R. Windmiller, Z. Fisk, R. F. Hoyt, A. C. Mota, and R. Viswanathan, *Int. J. Quantum Chem., Quantum Chem. Symp.* **9**, 569 (1975).
  - [11] H. R. Ott, M. Chernikov, E. Felder, L. Degiorgi, E. G. Moshopoulou, J. L. Sarrao, and Z. Fisk, *Z. Phys. B* **102**, 337 (1997).
  - [12] S. Massidda, A. Continenza, T. M. Pascale, and R. Monnier, *Z. Phys. B* **102**, 83 (1997).
  - [13] B. T. Matthias, *Phys. Lett.* **27A**, 511 (1968).
  - [14] M. C. Aronson, J. C. Cooley, J. Sarrao, and Z. Fisk (private communication).
  - [15] Z. Fisk, D. C. Johnston, B. Cornut, S. von Molnar, S. Oseroff, and R. Calvo, *J. Appl. Phys.* **50**, 1911 (1979).
  - [16] T. Fujita, M. Suzuki, and Y. Isikawa, *Solid State Commun.* **33**, 947 (1980).
  - [17] Y. Okimoto, T. Katsufuji, T. Ishikawa, T. Arima, and Y. Tokura, *Phys. Rev. B* **55**, 4206 (1997).
  - [18] T. Osafune, N. Motoyama, H. Eisaki, and S. Uchida, *Phys. Rev. Lett.* **78**, 1980 (1997).
  - [19] S. Kimura, T. Nanba, M. Tomikawa, S. Kunii, and T. Kasuya, *Phys. Rev. B* **46**, 12 196 (1992).
  - [20] F. Wooten, *Optical Properties of Solids* (Academic, New York, 1972).
  - [21] P. A. Alekseev, A. S. Ivanov, B. Dorner, H. Schober, K. A. Kikoin, A. S. Mishchenko, V. N. Lazukov, E. S. Konovalova, Yu. B. Paderno, A. Yu. Romyantsev, and I. P. Sadikov, *Europhys. Lett.* **10**, 457 (1989); P. Nyhus, S. L. Cooper, J. L. Sarrao, and Z. Fisk, *Phys. Rev. B* **52**, 14 308 (1995).
  - [22] Y. Okimoto, T. Katsufuji, T. Ishikawa, A. Urushibara, T. Arima, and Y. Tokura, *Phys. Rev. Lett.* **75**, 109 (1995).